Cell
P R E S S

Zinc Sequestration by the Neutrophil Protein Calprotectin Enhances *Salmonella* Growth in the Inflamed Gut

Janet Z. Liu,[1,2] Stefan Jellbauer,[1,2] Adam J. Poe,[1,2] Vivian Ton,[1,2] Michele Pesciaroli,[1,2,5] Thomas E. Kehl-Fie,[6]
Nicole A. Restrepo,[7] Martin P. Hosking,[2,3] Robert A. Edwards,[2,4] Andrea Battistoni,[8] Paolo Pasquali,[5] Thomas E. Lane,[2,3]
Walter J. Chazin,[7] Thomas Vogl,[9] Johannes Roth,[9] Eric P. Skaar,[6] and Manuela Raffatellu[1,2,*]
[1]Department of Microbiology and Molecular Genetics
[2]Institute for Immunology
[3]Department of Molecular Biology and Biochemistry
[4]Department of Pathology and Laboratory Medicine
University of California, Irvine, CA 92697, USA
[5]Department of Veterinary Public Health and Food Safety, Istituto Superiore di Sanità, Roma, Italy
[6]Department of Microbiology and Immunology, Vanderbilt University Medical School
[7]Departments of Biochemistry and Chemistry, Center for Structural Biology
Vanderbilt University, Nashville, TN 37232, USA
[8]Department of Biology, University of Rome Tor Vergata, Roma, Italy
[9]Institute of Immunology, University of Münster, Münster, Germany
*Correspondence: manuelar@uci.edu
DOI 10.1016/j.chom.2012.01.017

SUMMARY

Neutrophils are innate immune cells that counter pathogens by many mechanisms, including release of antimicrobial proteins such as calprotectin to inhibit bacterial growth. Calprotectin sequesters essential micronutrient metals such as zinc, thereby limiting their availability to microbes, a process termed nutritional immunity. We find that while calprotectin is induced by neutrophils during infection with the gut pathogen *Salmonella* Typhimurium, calprotectin-mediated metal sequestration does not inhibit *S.* Typhimurium proliferation. Remarkably, *S.* Typhimurium overcomes calprotectin-mediated zinc chelation by expressing a high affinity zinc transporter (ZnuABC). A *S.* Typhimurium *znuA* mutant impaired for growth in the inflamed gut was rescued in the absence of calprotectin. ZnuABC was also required to promote the growth of *S.* Typhimurium over that of competing commensal bacteria. Thus, our findings indicate that *Salmonella* thrives in the inflamed gut by overcoming the zinc sequestration of calprotectin and highlight the importance of zinc acquisition in bacterial intestinal colonization.

INTRODUCTION

Salmonella enterica serovar Typhimurium (*S.* Typhimurium) is a gut pathogen that causes an acute gastroenteritis characterized by inflammatory diarrhea. *S.* Typhimurium encodes two type III secretion systems (T3SS-1 and T3SS-2) that are important for eliciting intestinal inflammation (Hapfelmeier and

Hardt, 2005; Tsolis et al., 1999). Initiation of the inflammatory response in the gut requires interaction with host cells, including epithelial cells and antigen-presenting cells (APCs), like macrophages and dendritic cells. APCs infected with *S.* Typhimurium secrete several cytokines, including interleukin (IL)-23 and IL-18, which stimulate T cells in the intestinal mucosa to produce IL-17 and IL-22 (Godinez et al., 2008, 2009; Raffatellu et al., 2008; Srinivasan et al., 2007). These cytokines subsequently induce responses in the tissue that results in the influx of neutrophils to the gut mucosa, a hallmark of inflammatory diarrhea.

Neutrophils control *S.* Typhimurium dissemination, as inferred from clinical observations in patients with defects in neutrophil-killing mechanisms (for instance, chronic granulomatous disease patients) or neutropenia (Winkelstein et al., 2000). In these groups of patients, *S.* Typhimurium infection often disseminates from the gut, resulting in bacteremia and high mortality (Noriega et al., 1994). In response to *S.* Typhimurium infection, both neutrophils and epithelial cells secrete antimicrobial proteins into the intestinal lumen that may be responsible for the dramatic changes in the composition of the microbiota observed during *S.* Typhimurium infection (Barman et al., 2008; Lupp et al., 2007; Stecher et al., 2007). Furthermore, several recent studies have demonstrated that the host inflammatory response favors *S.* Typhimurium growth in the gut and its transmission to a naive host (Barman et al., 2008; Lawley et al., 2008; Lupp et al., 2007; Raffatellu et al., 2009; Stecher et al., 2007). Within this inflammatory environment, *S.* Typhimurium must acquire essential nutrients and anaerobically respire tetrathionate to successfully outgrow the resident microbiota (Raffatellu et al., 2009; Winter et al., 2010). *S.* Typhimurium must also be resistant to the inhibitory and lethal activities of antimicrobial proteins released into the lumen in response to infection, some of which may actually promote the growth of this pathogen over competing microbes that are susceptible to their activity.

The identity of many antimicrobial proteins secreted during *S.* Typhimurium infection, and whether these peptides are protective or promote pathogen growth, is largely unknown. Because the influx of neutrophils is a hallmark of *S.* Typhimurium diarrhea, antimicrobial proteins released by neutrophils are likely major players in the host response to *S.* Typhimurium. Calprotectin, a heterodimer of the two EF-hand calcium-binding proteins S100A8 and S100A9, is one of the most abundant antimicrobial proteins in neutrophils, constituting approximately 40% of cytoplasmic neutrophil content (Teigelkamp et al., 1991). This protein complex is secreted to high levels during inflammation (Steinbakk et al., 1990), and is associated with extracellular traps released by apoptotic neutrophils to kill microbes (Urban et al., 2009). Mucosal and skin epithelial cells stimulated with the cytokine IL-22 also express *S100a8* and *S100a9*, indicating that epithelial cells may also be a source of this antimicrobial protein (Liang et al., 2006; Zheng et al., 2008). Calprotectin has antimicrobial activity against many microorganisms, including *Escherichia coli*, *Borrelia burgdorferi*, *Staphylococcus aureus, Listeria monocytogenes*, and *Candida albicans* (Corbin et al., 2008; Loomans et al., 1998; Lusitani et al., 2003; Sohnle et al., 2000; Steinbakk et al., 1990; Urban et al., 2009; Zaia et al., 2009). This activity is dependent on the ability of calprotectin to bind nutrient metals such as zinc and manganese, thereby starving microbes of these essential metal ions (Corbin et al., 2008; Kehl-Fie et al., 2011; Urban et al., 2009). With regard to the intestine, fecal calprotectin levels are used clinically to monitor the severity of intestinal inflammation in patients with inflammatory bowel diseases (Konikoff and Denson, 2006). Despite these observations, the role of calprotectin in the intestinal inflammatory response during infection with gut pathogens is largely unknown. In this study, we set out to determine the role of the antimicrobial protein calprotectin during infection with *S.* Typhimurium as a model for inflammatory diarrhea.

RESULTS

Calprotectin Expression in the Cecum during Infection with *S.* Typhimurium

Our previous studies indicated that the two subunits of calprotectin, *S100a8* and *S100a9*, are among the highest upregulated genes during infection with *S.* Typhimurium in the ileum of rhesus macaques and in the cecum of mice (Godinez et al., 2008; Raffatellu et al., 2008). To further confirm these observations, we employed the streptomycin-pretreated mouse colitis model of *S.* Typhimurium infection, which results in acute inflammation of the cecal mucosa characterized by an influx of neutrophils (Barthel et al., 2003; Raffatellu et al., 2009). Using this model, we found that calprotectin was highly induced in the cecum and fecal samples of mice infected with *S.* Typhimurium compared to mock-infected mice (Figure 1). The mRNA for the two subunits of calprotectin, *S100a8* and *S100a9*, was significantly upregulated at both day 3 (Figure 1A) and day 4 post infection (Figure 1B). We next extracted total protein from fecal samples (Figure 1C) and the large intestine (Figure 1D) of mock- or *S.* Typhimurium-infected mice and then determined calprotectin concentration by ELISA. We detected a significant increase in the expression of calprotectin in both the fecal samples and in the tissue of the large intestine after *S.* Typhimurium infection, with average concentrations being 130 μg/ml and 793 μg/ml respectively. Because intestinal epithelial cells may express antimicrobial peptides, we next determined whether crypt colonocytes could be a source of calprotectin.

Mice were infected with either *S.* Typhimurium or mock and we isolated crypt cells from the large intestine (Figure S1). As a positive control, we confirmed that crypt colonocytes isolated from mice infected with *S.* Typhimurium exhibited an increase in the expression of the antimicrobial peptide lipocalin-2, which is induced in epithelial cells during infection (Raffatellu et al., 2009). In addition, we detected increased expression of the *S100a8* and *S100a9* subunits, indicating that these cells may also be a source of calprotectin (Figure 1E). As the increase in calprotectin correlated with the increased inflammatory response and the influx of neutrophils in these mice, we questioned to what extent neutrophils and epithelial cells contribute to the increase of calprotectin expression observed during *S.* Typhimurium infection.

To test this, we infected mice treated with an antibody against the neutrophil receptor Cxcr2 (Figure 2). The Cxcr2 receptor binds to the chemokine *Cxcl-1* expressed in the inflamed gut, thereby promoting the transmigration of neutrophils to the site of infection. Blocking the Cxcr2 receptor reduces neutrophil transmigration to the infected tissue and depletes neutrophils from the blood, as previously described by Hosking et al. (2009). As a control, mice were injected with normal rabbit serum (NRS). To test the effectiveness of our neutrophil depletion, we detected the CD11b$^+$ Ly6g^{high} cells (neutrophils) in the blood collected from the NRS-treated and the anti-Cxcr2-treated mice by flow cytometry. As expected, treatment with the anti-Cxcr2 antibody reduced the amount of neutrophils in the blood (Figure 2B). To determine the contribution of neutrophils and colonocytes to the expression of calprotectin during infection, we extracted both RNA and protein from the cecum (Figures 2C and 2D) and the crypt colonocytes (Figures 2E and 2F) of the NRS-treated and the anti-Cxcr2-treated mice. Our results indicate that in mice treated with the anti-Cxcr2 antibody, there was only a minor reduction in the expression of *S100a8* and *S100a9* mRNA in comparison to the NRS-treated mice in the cecum (Figure 2C) and no reduction in the crypt colonocytes (Figure 2E). Thus, neutrophils appear to be dispensable for the induction of *S100a8* and *S100a9* transcription in crypt colonocytes. In contrast, mice treated with the anti-Cxcr2 antibody exhibited a marked reduction in the expression of calprotectin at the protein level, which correlated with the reduction of the neutrophil marker myeloperoxydase (MPO) in these mice (Figure 2D). Moreover, we did not detect high levels of calprotectin expression at the protein level in crypt colonocytes—the low level of expression was likely due to contamination with neutrophils, as indicated by the detection of MPO (Figure 2F). Therefore, although transcription of *S100a8* and *S100a9* is highly induced in colonocytes, neutrophils appear to be the major source of calprotectin protein. Taken together, our results indicate that calprotectin is expressed at high levels in the large intestine during *S.* Typhimurium infection, suggesting that it may play an important role in the host response to this infection.
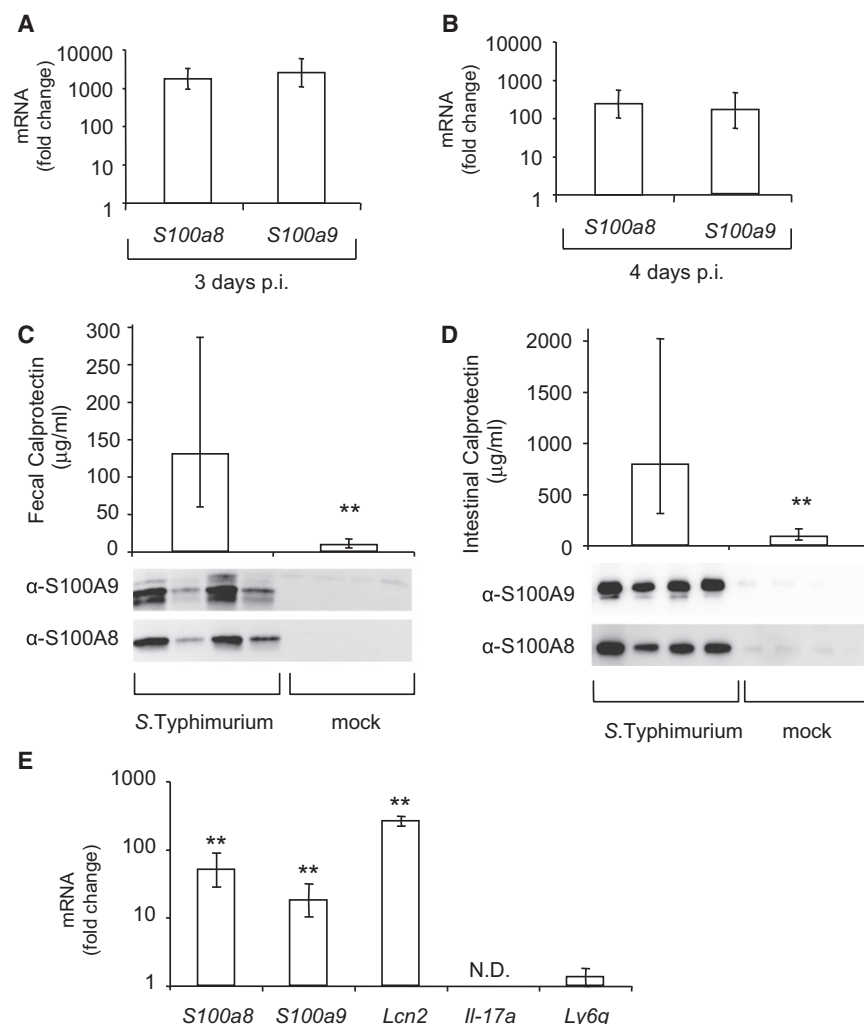
Figure 1. Expression of Calprotectin in the Cecum of Mice Infected with S. Typhimurium

(A and B) *S100a8* and *S100a9* were detected by RT-PCR at 72 hr (A) and 96 hr (B) after infection with wild-type *S.* Typhimurium. Data are expressed as fold increase over mock-infected wild-type mice. Bars represent the geometric means ± standard error.

(C and D) The concentration of calprotectin detected by ELISA (top panel) and western blot (bottom panel) in the fecal samples (C) and the large intestine with content (D) of mice 96 hr post infection with *S.* Typhimurium (n = 4) or mock control (n = 4) is shown. Bars represent the geometric mean ± standard deviation. ** p value ≤ 0.01.

(E) Expression of the *S100a8* and *S100a9* mRNAs was detected in crypt colonocytes isolated from the colon of mice infected with *S.* Typhimurium (n = 3) and expressed as fold increase over mock-infected mice (n = 3). Expression of *Lcn2* was detected as a positive control and of the T cell cytokine *Il-17a* and the neutrophil marker *Ly6g* as a negative control. ND = not detected. Data represent the geometric mean ± standard error. A significant increase over mock control is indicated by * (p value ≤ 0.05) and ** (p value ≤ 0.01). (See also Figure S1 and Table S1).

confirmed that our *znuA* mutant had a growth defect in minimal media that could be rescued by supplementation with zinc sulfate, as previously shown (Ammendola et al., 2007) (Figure S2). When we grew the *znuA* mutant in rich media supplemented with calprotectin, we found that its growth was impaired at concentrations of calprotectin where wild-type is only minimally inhibited (approximately 125 μg/ml) (Figure 3B). Thus, the ability to acquire zinc through the ZnuABC transporter renders *S.* Typhimurium more resistant to the antimicrobial activity of calprotectin in vitro. Our results thus far suggested that the calprotectin level encountered by *S.* Typhimurium in the intestinal lumen has only minimal activity against the organism and that zinc acquisition through ZnuABC may render this pathogen resistant to this protein in vivo.

The ZnuABC Zinc Transporter Promotes S. Typhimurium Colonization of the Inflamed Cecum

To assess whether high affinity zinc transporters may provide an advantage in the gut environment, we first determined the concentration of zinc in the feces of mice infected with *S.* Typhimurium or mock by inductively coupled plasma mass spectrometry (ICP-MS) (Figure 4). We found that the concentration of fecal zinc in the absence of infection was about 220 mg/kg, while it was reduced to 56 mg/kg in infected mice (Figure 4A). Therefore, the lower levels of zinc in the inflamed gut suggested that the expression of a high affinity zinc transporter may provide a growth advantage for colonization. To test this, we next investigated whether inactivation of the *znuA*

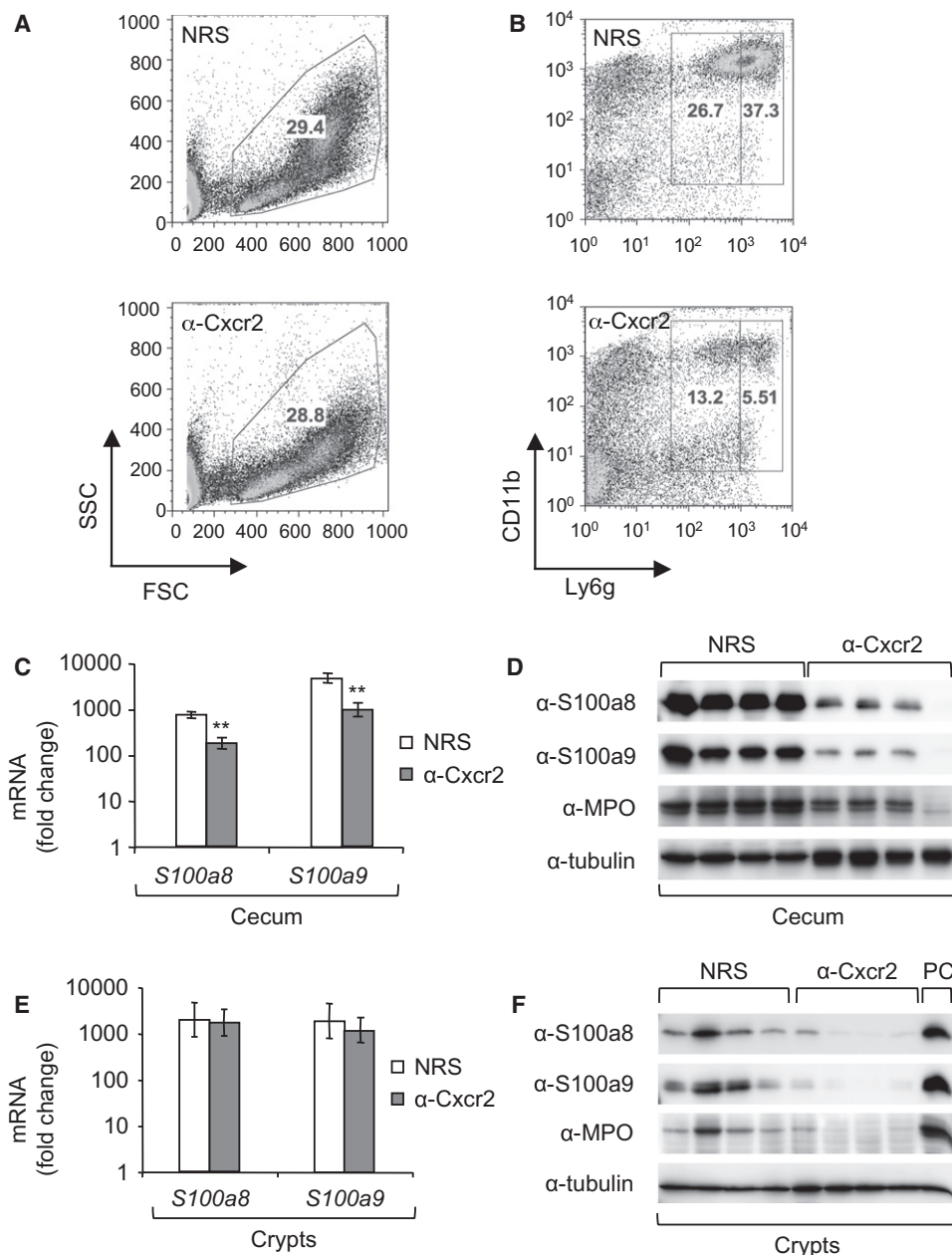## Growth of S. Typhimurium in Rich Media Supplemented with Calprotectin

To investigate the role of calprotectin during *S.* Typhimurium infection, we next determined whether calprotectin was able to reduce the growth of *S.* Typhimurium. We performed a growth assay of *S.* Typhimurium in rich media supplemented with purified calprotectin (Figure 3). When calprotectin was added at a concentration typical of a tissue abscess (500 μg/ml) (Johne et al., 1997), *S.* Typhimurium growth was inhibited. In contrast, lower concentrations of calprotectin, comparable to that measured in the fecal samples of infected animals (Figure 1C), only minimally reduced *S.* Typhimurium growth (Figure 3A), indicating that *Salmonella* could potentially defend against this insult in the intestinal lumen. We then looked to determine the mechanism by which *S.* Typhimurium grew in the media supplemented with calprotectin.

Because calprotectin is known to chelate zinc ions, we hypothesized that *S.* Typhimurium growth was dependent on the high affinity zinc transporter encoded by the *znuABC* operon, which is induced in zinc-limiting conditions (Ammendola et al., 2007; Campoy et al., 2002). We subsequently deleted the gene encoding the periplasmic zinc-binding component, *znuA*, and

Figure 2. Expression of Calprotectin in Mice following Neutrophil Depletion

Mice were injected intraperitoneally with either normal rabbit serum (NRS) or a rabbit polyclonal antibody blocking the Cxcr2 receptor (α-Cxcr2) 24 hr prior to infection with *S.* Typhimurium and sacrificed at 72 hr post infection. (A) shows a representative dot plot (FSC = forward scatter; SSC = side scatter) of blood cells gated on leucocytes from mice treated with NRS (top) and α-Cxcr2 (bottom). (B) shows a representative dot plot of blood leucocytes gated on neutrophils expressing Ly6g and CD11b from mice treated with NRS (top) and α-Cxcr2 (bottom). In (C and D), cecal expression of the S100a8 and the S100a9 subunits of calprotectin was detected by real-time RT-PCR (C) and western blot (D). In (E and F), crypt expression of the S100a8 and the S100a9 subunits of calprotectin was detected by real-time RT-PCR (E) and western blot (F); MPO = myeloperoxidase; PC = positive control. Data represent the geometric mean ± standard error. A significant difference in expression between NRS-treated and α-Cxcr2-treated mice is indicated by ** (p value ≤ 0.01).

gene would impair the ability of *S.* Typhimurium to colonize the intestine. *S.* Typhimurium infection results in intestinal inflammation, which is facilitated by the actions of two type III secretion systems encoded by *Salmonella* pathogenicity islands (SPI)-1 and SPI-2 (Santos et al., 2009). Inactivation of both secretion systems through deletion of the *invA* and *spiB* genes, respec-

tively, renders *S.* Typhimurium unable to elicit colitis in mice (Raffatellu et al., 2009; Stecher et al., 2007). We thus compared groups of mice infected with *S.* Typhimurium wild-type, the *znuA* mutant, or a mutant lacking both the *invA* and *spiB* genes. The *znuA* mutant triggered similar levels of inflammation and expression of calprotectin and cytokines in the cecum as
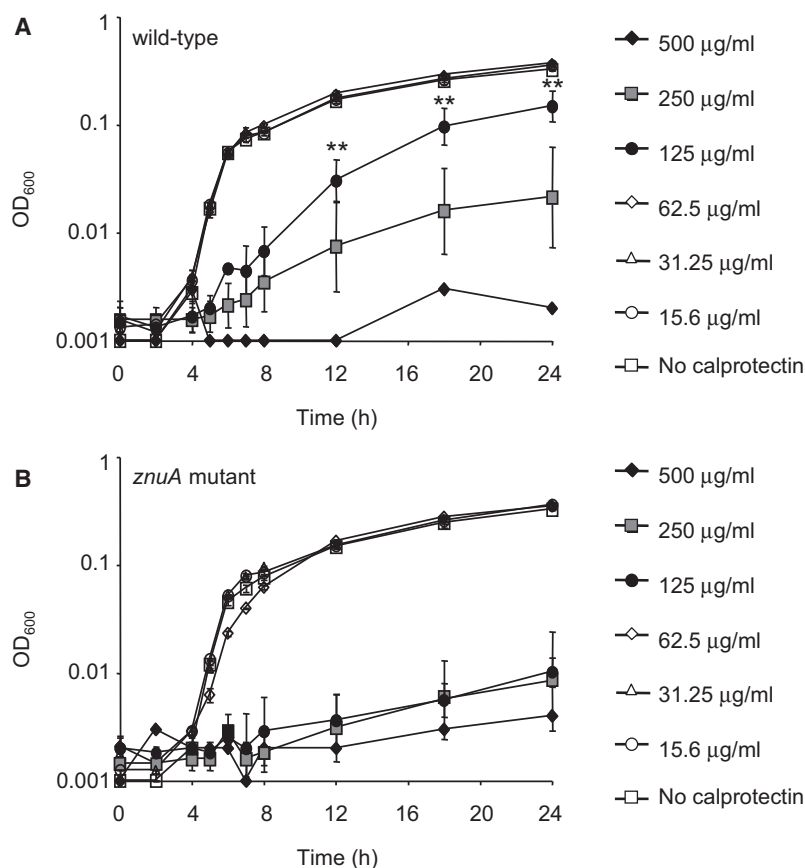
Figure 3. Growth of *S.* Typhimurium in Rich Media Supplemented with Calprotectin

(A and B) *S.* Typhimurium wild-type (A) or the *znuA* mutant (B) were grown in LB media supplemented with calprotectin at the indicated concentrations. Growth was determined by reading the OD_{600} in a microplate reader at the indicated times. Data represent the geometric mean of four biological replicates ± standard error. A significant difference in growth between wild-type and the *znuA* mutant is indicated by ** (p value ≤ 0.01). (See also Figure S2 and Table S2).

Clostridiales similar to wild-type. However, the *znuA* mutant exhibited a markedly reduced ability to take advantage of the decrease in competing microbes, and it colonized to similar levels as the *invA spiB* mutant (Figures 4E and 4F). Intriguingly, while administration of zinc to mice in the form of zinc sulfate enhanced the growth of *S.* Typhimurium wild-type, it did not rescue the *znuA* mutant (Figures 4E and 4F). One plausible explanation is that administration of zinc sulfate may promote the growth of other bacterial species that are more fit than the *znuA* mutant to colonize this environment. To test this possibility, we analyzed the microbiota in stool samples of mice supplemented with zinc sulfate infected with the *znuA* mutant. While we observed low levels of *Bacteroidetes* and *Clostridiales*, we also detected a significant increase in *Enterobacteriaceae* other than *Salmonella* species, which may account at least partly for the reduced ability of the *znuA* mutant to proliferate in this environment. Moreover, we did not detect an increase in other *Enterobacteriaceae* in mock-infected or wild-type-infected mice supplemented with zinc sulfate (data not shown). These results indicate that the ZnuABC transporter aids in competing with the microbiota and promotes *S.* Typhimurium colonization of the cecum.

Resistance to Calprotectin-Mediated Zinc Sequestration Provides a Growth Advantage to *S.* Typhimurium

To test if zinc acquisition and resistance to calprotectin would increase *S.* Typhimurium fitness in vivo, we infected mice with an equal mixture of *S.* Typhimurium wild-type and the *znuA* mutant (Figures 5–7, S4, and S5). In this experimental setting, the ability of the *znuA* mutant and of wild-type to colonize the intestine is compared in each individual animal (i.e., in the same gut environment), thereby reducing the effect of animal-to-animal variation observed in single infections. *S.* Typhimurium infection resulted in increased cecal inflammation and an influx of neutrophils (Figures 5 and S4), which correlated with increased transcript levels of the neutrophil chemoattractant *Cxcl-1* (Figure 5B) and the neutrophil marker *Ly6g* (Figure 5C). Moreover, the transcript levels of the proinflammatory cytokines *Il-17a* and *Il-22* were also increased (Figure S4). These data confirmed that *S.* Typhimurium infection was associated with acute cecal inflammation and neutrophil influx. The transcript

observed with the wild-type strain, indicating that this mutant retained virulence (Figures 4B–4D and S3). However, colonization of the *znuA* mutant was reduced approximately 200 fold at 96 hr post infection to levels similar to an avirulent *S.* Typhimurium strain lacking *invA* and *spiB* (Figure 4E).
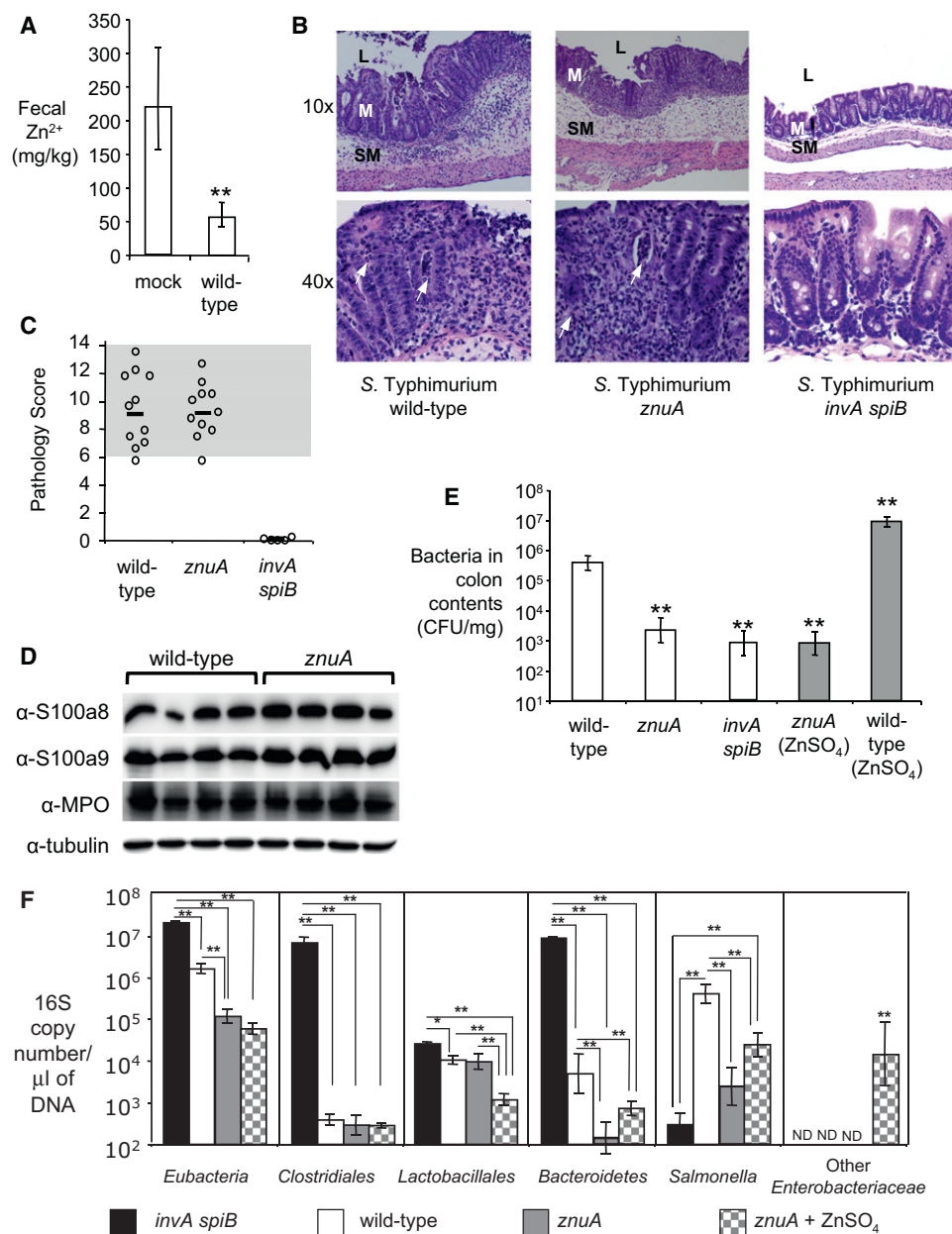
In recent years, several studies have demonstrated that *S.* Typhimurium and other gut pathogens benefit from inflammation because they have to compete with the resident microbiota to colonize the inflamed gut (Barman et al., 2008; Lawley et al., 2008; Lupp et al., 2007; Stecher et al., 2007; Winter et al., 2010). It is known that the *invA spiB* mutant does not colonize as well as wild-type because it does not trigger an inflammatory response and it is therefore outcompeted by the microbiota (Lawley et al., 2008; Raffatellu et al., 2009; Stecher et al., 2007; Winter et al., 2010). Because the *znuA* mutant showed a striking colonization defect despite eliciting inflammation, we hypothesized that this strain is less fit than wild-type to sustain competition with the microbiota.

Analysis of the microbiota in stool samples of mice infected with the *znuA* mutant confirmed this prediction (Figure 4F). Infection with *S.* Typhimurium wild-type, but not the *invA spiB* mutant, induced a loss of *Bacteroidetes* and *Clostridiales*, as previously described (Barman et al., 2008; Lawley et al., 2008; Lupp et al., 2007; Stecher et al., 2007; Winter et al., 2010). Therefore, *S.* Typhimurium wild-type but not the *invA spiB* mutant, was able to outcompete the microbiota (Figures 4E and 4F). Remarkably, the *znuA* mutant induced a loss of *Bacteroidetes* and

Figure 4. The ZnuABC Zinc Transporter Promotes *S.* Typhimurium Colonization of the Inflamed Cecum

(A) The concentration of zinc was measured by ICP-MS in fecal samples collected from mock-infected (n = 4) or *S.* Typhimurium-infected (n = 4) mice 4 days post infection. Bars represent geometric means ± standard deviation. A significant difference is indicated by ** (p value ≤ 0.01).

(B and C) Histopathology of cecal samples collected from mice 4 days after infection with *S.* Typhimurium wild-type, the *znuA* mutant, or the *invA spiB* mutant. (B) H&E-stained cecal sections from representative animals in each group. An image at lower magnification (10×) and one at higher magnification (40×) from the same section are shown. L = lumen; M = mucosa; SM = submucosa. Note marked edema in the submucosa and inflammation in mice infected with both *S.* Typhimurium wild-type and the *znuA* mutant. (C) Blinded histopathology score indicating the score of individual mice (circles), and the average score for each group (bars). The gray quadrant includes scores indicative of moderate to severe inflammation.

(D) S100a8, S100a9, myeloperoxidase (MPO), and tubulin were detected by immunoblot in the cecum of mice infected with *S.* Typhimurium wild-type or the *znuA* mutant.

(E and F) (E) shows enumeration of *S.* Typhimurium in the colon content (wild-type n = 11, *znuA* mutant n = 11, *invA spiB* mutant n = 6; *znuA*+ZnSO₄ n = 9; wild-type+ZnSO₄ n = 6). (F) Analysis of the cecal microbiota using 16S rRNA gene qRT-PCR (wild-type n = 10, *znuA* mutant n = 9, *invA spiB* mutant n = 6; *znuA*+ZnSO₄ n = 9). For (E and F), bars represent geometric means ± standard error. In (A and E), a significant difference in comparison to wild-type infected mice is indicated by ** (p value ≤ 0.01). (F) Significant differences between groups are indicated by * (p value ≤ 0.05) and ** (p value ≤ 0.01). (See also Figure S3 and Table S3).
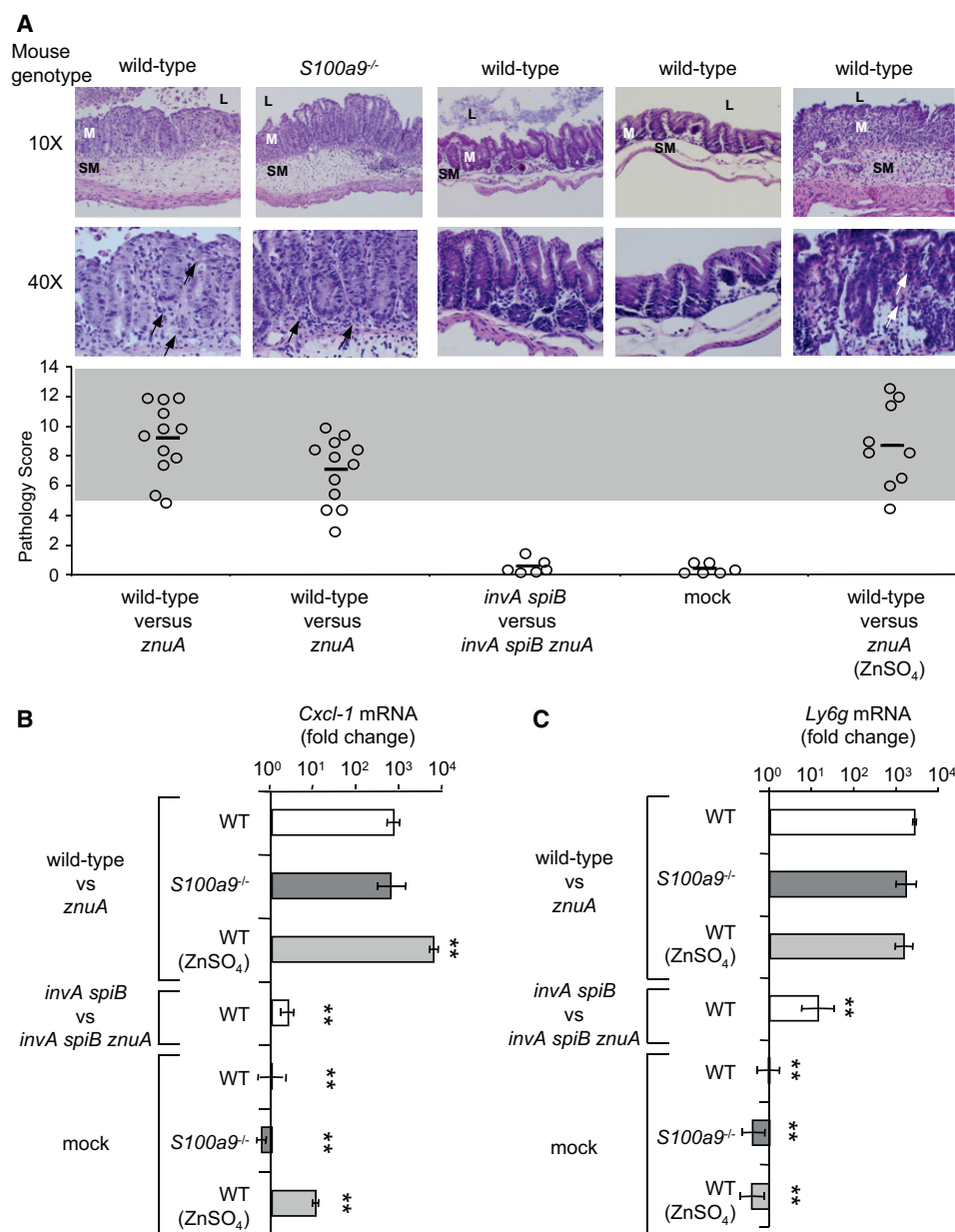
Figure 5. Analysis of the Host Response in Mice Infected with *S.* Typhimurium, Wild-Type + *znuA* Mutant, or Mock

(A) Histopathology of the cecum. Upper panels: H&E-stained cecal sections from representative animals in each group. An image at lower magnification (10×) and one at higher magnification (40×) from the same section are shown. L = lumen; M = mucosa; SM = submucosa. Note marked edema in the submucosa and inflammation in infected mice. Lower panel: blinded histopathology scores, indicating the score of individual mice (circles), and the average score for each group (bars). The gray quadrant includes scores indicative of moderate to severe inflammation.

(B and C) Transcript levels of *Cxcl-1* (B) and *Ly6g* (C), were determined in wild-type mice (white bars), $S100a9^{-/-}$ mice (dark gray bars), and wild-type mice supplemented with zinc sulfate (light gray bars). Mice were either mock-infected or infected with *S.* Typhimurium as indicated. Data are expressed as fold increase over mock-infected wild-type mice. Bars represent the geometric mean of at least 4 replicates ± standard error. Significant differences in gene expression in comparison to wild-type infected C57BL/6 mice (first group) are indicated by ** (p value ≤ 0.01). (See also Figure S4).

levels of the two subunits of calprotectin *S100a8* and *S100a9* were also determined to be highly induced (Figures 6A and 6B). While no calprotectin was detected in the cecal mucosa of mock-infected mice, the protein complex was highly abundant after *S.* Typhimurium infection, and it correlated with the increase in MPO levels (Figure 6C). In this gut environment with high levels

of inflammation and calprotectin, we observed a marked increase in *S.* Typhimurium wild-type over the *znuA* mutant at days 3 and 4 post infection (average of 87-fold and 690-fold, respectively), suggesting that zinc acquisition through the ZnuABC transporter enhances *S.* Typhimurium growth in the inflamed gut (Figures 7A and 7B).
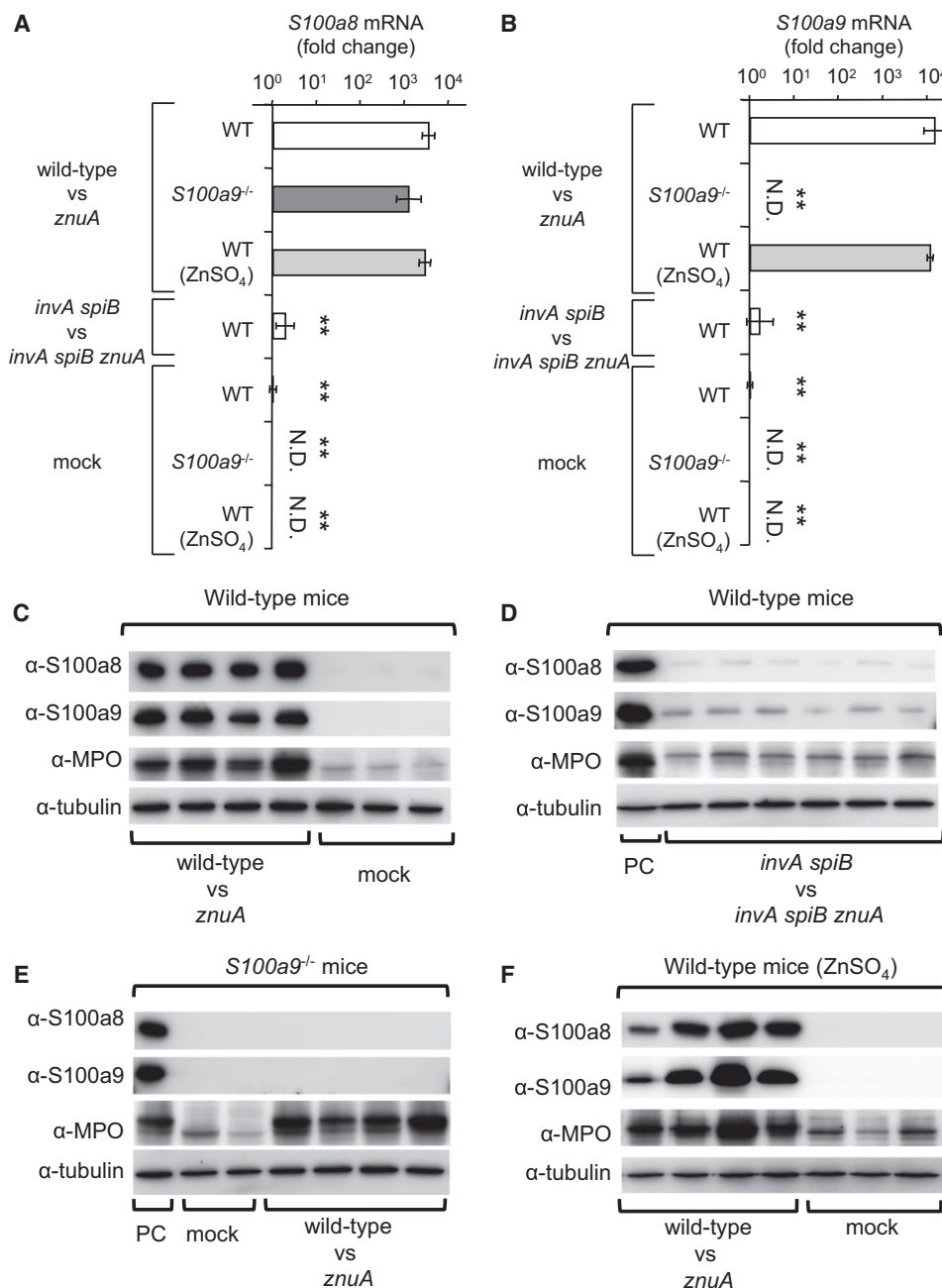
**Figure 6. Calprotectin Expression in the Cecum Detected by Quantitative Real-Time PCR and Western Blot**

(A and B) Transcript levels of *S100a8* (A) and *S100a9* (B) were determined in wild-type mice (white bars), *S100a9*$^{-/-}$ mice (dark gray bars), and wild-type mice supplemented with zinc sulfate (light gray bars). Mice were either mock-infected or infected with *S.* Typhimurium as indicated. Bars represent the geometric mean of at least four replicates ± standard error. Significant differences in gene expression in comparison to wild-type infected C57BL/6 mice (first group) are indicated by * (p value ≤ 0.05) and ** (p value ≤ 0.01).

(C–F) S100a8, S100a9, myeloperoxidase (MPO), and tubulin were detected by immunoblot in the cecum of mice infected with *S.* Typhimurium. Strain and mouse genotypes are indicated. PC = positive control.

We next sought to determine whether zinc acquisition through the ZnuABC transporter was significant in the absence of gut inflammation. To determine if the ZnuABC transporter provides a growth advantage in the absence of inflammation, we infected mice with an equal mixture of an *invA spiB* mutant and an *invA spiB znuA* mutant (Figures 5–7, S4, and S5). As expected, these

mice exhibited minimal or no intestinal inflammation (Figures 5A and S4), and the transcript levels for the neutrophil chemoattractant *Cxcl-1*, the neutrophil marker *Ly6g* and the proinflammatory cytokines *Il-17* and *Il-22* were increased only minimally when compared to mock-infected animals (Figures 5B, 5C, and S4). Increased expression of the two subunits of calprotectin,
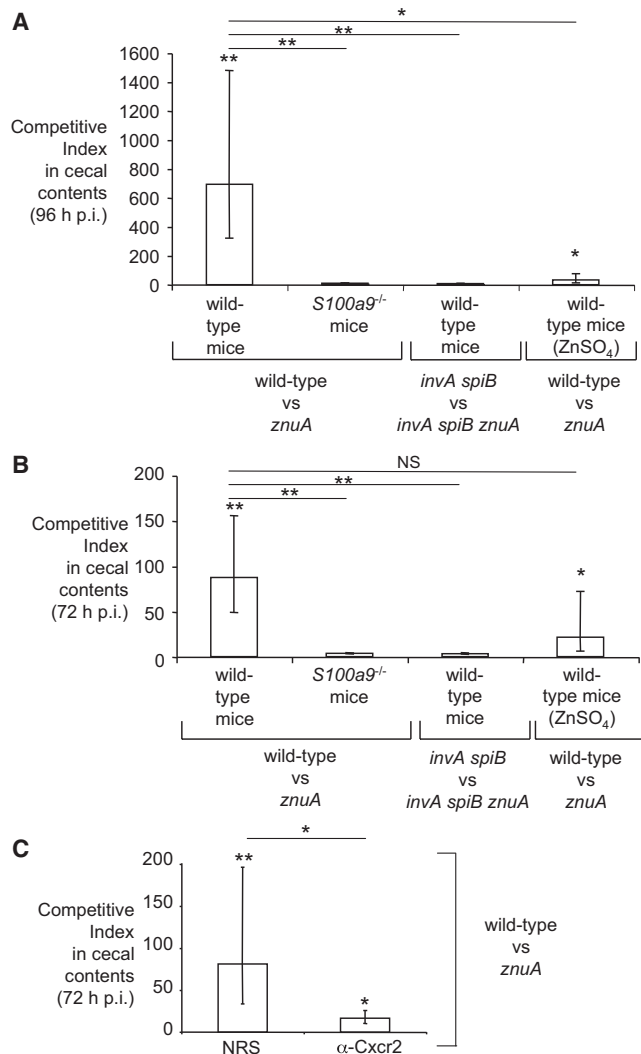
Figure 7. Resistance to Calprotectin-Mediated Zinc Sequestration Provides a Growth Advantage to *S.* Typhimurium

Cecal samples were collected from mice 3–4 days after infection with either *S.* Typhimurium or mock control. Competitive index was calculated by dividing the output ratio (CFU of the wild-type /CFU of the mutant) by the input ratio (CFU of the wild-type /CFU of the mutant). (A–C) show competitive indices of *S.* Typhimurium strains in the colon contents of mice (n ≥ 6/group) at 4 days (A) or 3 days (B) post infection. Strain and mouse genotypes are indicated. In (C), competitive index in cecal content of mice treated with either normal rabbit serum (NRS) or a rabbit polyclonal antibody blocking the Cxcr2 receptor (α-Cxcr2) at 72 hr post infection is shown. Bars represent geometric mean ± standard error. Significant differences are indicated by * (p value ≤ 0.05) and ** (p value ≤ 0.01). (See also Figure S5).

S100a8 and *S100a9,* was not detectable by quantitative real-time PCR, and little calprotectin and MPO expression was found by western blot (Figure 6D). Importantly, in this mixed infection, the *invA spiB* mutant and the *invA spiB znuA* mutant were recovered at nearly equal ratios at both 72 hr and 96 hr post infection, indicating that the *znuA* mutant is still capable of growing to similar levels as wild-type in the intestinal lumen under noninflammatory conditions (Figures 7A and 7B). Because neutrophils are a major source of calprotectin, we infected mice treated with

an antibody against Cxcr2 with a mixture of *S.* Typhimurium wild-type and the *znuA* mutant. As a control, mice were injected with normal rabbit serum (NRS). In the NRS-treated mice, where calprotectin was expressed to similar levels as in wild-type mice, we recovered 80-fold more *S.* Typhimurium wild-type than the *znuA* mutant at 72 hr post infection (Figure 7C), which is comparable to what we observed in wild-type (not NRS-treated) mice at the same time point (Figure 7B). In contrast, the growth disadvantage of the *znuA* mutant was reduced in mice treated with an antibody against Cxcr2 (Figure 7C), which showed reduced calprotectin expression (Figure 2). These data indicate that only during inflammation is zinc acquisition through the ZnuABC transporter seen to provide a growth advantage.

Next, we investigated whether the growth benefit provided by intestinal inflammation to *S.* Typhimurium wild-type was dependent on the expression of calprotectin. To assess this, we employed $S100a9^{-/-}$ mice, which lack the expression of both the S100a8 and S100a9 subunits of calprotectin due to decreased stability of S100a8 at the protein level in the absence of its binding partner S100a9 (Manitz et al., 2003) (Figure 6). The $S100a9^{-/-}$ mice were infected with an equal mixture of *S.* Typhimurium wild-type and the *znuA* mutant (Figures 5–7, S4, and S5), resulting in similar levels of colonization, inflammatory changes and MPO expression in tissue equivalent to wild-type mice (Figures 5,6, and S5). Moreover, infection of $S100a9^{-/-}$ mice resulted in an increase in expression of the proinflammatory markers *Cxcl-1*, *Ly6g*, *Il-17*, and *Il-22* comparable to that in wild-type mice (Figures 5B, 5C, and S4). Importantly, *S.* Typhimurium wild-type and the *znuA* mutant were recovered at nearly equal ratios at 72 hr and 96 hr post infection (Figures 7A and 7B). Taken together, these results indicate that sequestration of zinc ions by calprotectin provides a growth advantage to *S.* Typhimurium over an isogenic strain lacking the ability to acquire zinc via the ZnuABC transporter.

Next, we tested whether we could rescue the *znuA* mutant by administering zinc sulfate to mice infected with an equal mixture of *S.* Typhimurium wild-type and the *znuA* mutant. Infected mice receiving zinc sulfate via oral gavage through the course of the infection displayed similar levels of inflammation as wild-type mice (Figures 5 and S4). Furthermore, zinc supplementation did not result in significant changes in the expression of the proinflammatory genes *Il-17*, *Il-22*, or *Ly6g*, with the exception of the basal expression of *Cxcl-1* (Figures 5B, 5C, and S4). Similar to what we observed in the single infection in Figure 4E, zinc administration promoted a significant increase in overall *S.* Typhimurium colonization at both 72 hr and 96 hr post infection (Figure S5). Importantly, administration of zinc sulfate significantly reduced the growth disadvantage of the *znuA* mutant at 96 hr post infection (Figure 7A). Combined with our results of zinc supplementation in mice infected with the *znuA* mutant alone (Figures 4D and 4E), it emerges that the administration of zinc sulfate was able to rescue the *znuA* mutant in vivo only when the wild-type was also present (Figure 7A). These results suggest that wild-type may provide some cross-protection to the mutant in the mixed infection, either directly or indirectly by reducing the growth of competing microbes, and further underline the importance of an intact ZnuABC transporter during *S.* Typhimurium infection. Overall, our findings indicate that resistance to calprotectin, mediated by the capacity to acquire

zinc through the ZnuABC transporter, promotes *S.* Typhimurium competition in the inflamed gut.

DISCUSSION

One strategy a host employs in response to bacterial infection is to inhibit bacterial growth by limiting the availability of essential metal ions, a process known as nutritional immunity (Kehl-Fie and Skaar, 2010). However, with the exception of iron, the role of metal sequestration in response to pathogens is not thoroughly understood; evidence for the importance of zinc acquisition at the host-pathogen interface comes largely from studies on high affinity zinc transporters in bacteria. Furthermore, only a few studies have investigated the contribution of zinc transporters to bacterial pathogenesis.

The ZnuABC zinc transporter and the zinc uptake regulator Zur were originally described in *Escherichia coli* as a system for acquiring zinc under zinc-limiting conditions, subsequently being identified in several species of Gram-negative bacteria (Hantke, 2001). ZnuABC mutants are attenuated in mice that develop a systemic disease when infected with pathogens including *Brucella abortus*, *Pasteurella multocida*, and the typhoid model of *S.* Typhimurium (Ammendola et al., 2007; Campoy et al., 2002; Garrido et al., 2003; Kim et al., 2004). ZnuABC has also been found to play an important role in the pathogenesis of a variety of localized infections: In the rabbit model for chancroid, a *Haemophilus ducreyi znuA* mutant is less virulent and is rapidly cleared from lesions (Lewis et al., 1999); In mice infected with uropathogenic *E. coli* and *Proteus mirabilis*, while the ZnuABC transporter is not required for colonization of the bladder in single infections, it does provide an advantage in competitive experiments (Nielubowicz et al., 2010; Sabri et al., 2009); In chickens infected with *Campylobacter jejuni*, gastrointestinal colonization is dependent on a zinc transporter whose periplasmic component is an ortholog of *E. coli znuA* (Davis et al., 2009). However, despite experimental evidence indicating that the ZnuABC zinc transporter may promote colonization by several pathogens, little is known about the nutritional immune responses that induce zinc starvation in vivo.

The antimicrobial protein calprotectin, whose activity is dependent on zinc and manganese binding, is induced during bacterial and fungal infections in response to the cytokines IL-17 and IL-22 (Conti et al., 2009; Corbin et al., 2008; Kehl-Fie et al., 2011; Liang et al., 2006; Urban et al., 2009; Zheng et al., 2008). Our research shows that calprotectin is upregulated in the intestine in response to acute infection with *S.* Typhimurium (colitis model) and can be detected in the feces, consistent with findings that calprotectin is present in the feces of patients with intestinal inflammatory conditions, including inflammatory bowel diseases and colon cancer (Johne et al., 1997; Konikoff and Denson, 2006). Remarkably, whereas with other pathogens calprotectin-mediated zinc sequestration is necessary to suppress microbial growth (Corbin et al., 2008; Kehl-Fie et al., 2011; Urban et al., 2009), the growth of *S.* Typhimurium is actually enhanced over competing microbes by calprotectin expression. Importantly, we found that the ZnuABC zinc transporter conferred a significant advantage to *S.* Typhimurium in colonizing the gut when calprotectin is highly expressed (i.e, when the gut is inflamed). Consistent with this, in the absence of an inflammatory response or in mice lacking calprotectin, the ZnuABC transporter did not provide a colonization advantage. Therefore, our results indicate that zinc acquisition via the ZnuABC transporter facilitates *S.* Typhimurium growth in the inflamed gut by overcoming calprotectin-mediated zinc starvation. Remarkably, our work suggests that calprotectin enhances the competitive advantage of a pathogen and provides a mechanistic link between the ZnuABC transporter and a host zinc-limiting factor.

In conjunction with these insights, our study also underlines the acquisition of the micronutrient zinc in the inflamed gut as an important means of growth and competition between microbes. It is becoming more and more apparent that, in order to survive in a host, pathogens must contend with the resident microbiota for nutrients, often acquiring and evolving specialized systems to gain an advantage (Rohmer et al., 2011). In addition to overcoming calprotectin-mediated zinc sequestration, *S.* Typhimurium can also bypass lipocalin-2-mediated iron starvation in the inflamed gut by employing modified siderophores (Raffatellu et al., 2009). Together, these findings indicate that resistance to metal withholding responses may represent a common theme for pathogens to compete with the intestinal microbiota when colonizing the inflamed gut mucosa. Moreover, some species of commensal microbes in the gut may utilize metal transporters to grow under metal-limiting conditions. Future analyses of the distribution and function of metal transporters may provide useful insight into the life of microbial communities in the inflamed gut environment.

As the inflammatory host response is also essential for controlling the dissemination of *S.* Typhimurium, therapeutic interventions to limit intestinal inflammation and thus reduce the growth and transmission of this pathogen are not feasible. However, targeting a variety of bacterial metal acquisition systems may represent a promising strategy to limit infections with *S.* Typhimurium and other pathogens.

EXPERIMENTAL PROCEDURES

Bacterial Strains and Growth Conditions
IR715 is a fully virulent, nalidixic acid-resistant derivative of *S.* Typhimurium wild-type isolate ATCC 14028. Construction of IR715 derivatives carrying mutations in *znuA*, *invA*, or *spiB* is described in the Supplemental Experimental Procedures. A complete list of strains, plasmids, and primers used for cloning and strain construction is provided in Supplemental Experimental Procedures. All strains were grown aerobically at 37°C in Luria-Bertani (LB) broth unless otherwise noted.

Growth in Media Supplemented with Calprotectin
Recombinant calprotectin was produced as described elsewhere (Hunter and Chazin, 1998). Growth in media supplemented with calprotectin was performed as described by Kehl-Fie et al. (2011) with minor modifications (details in the Supplemental Experimental Procedures). Wild-type and *znuA S.* Typhimurium were grown overnight in M9 minimal media at 37°C with agitation. 1×10^5 cells/ml were used to inoculate the wells containing LB+calprotectin at the indicated concentrations. OD_{600} were taken at the indicated times and graphed on a semilogarithmic scale.

Mouse Experiments
Both C57BL/6 wild-type mice and S100A9$^{-/-}$ mice were used. The construction of S100A9$^{-/-}$ mice is described in the Supplemental Experimental Procedures. Mice were infected as previously described (Raffatellu et al., 2009). All animal experiments were reviewed and approved by the Institutional Animal Care and Use Committee at the University of California, Irvine.

Isolation of Colon Crypts

Streptomycin-treated C57BL/6 mice were infected with *S.* Typhimurium or mock and sacrificed at 72 hr post infection. Crypt isolation from colon and cecum was performed as described (Whitehead et al., 1993).

CXCR2 Antibody Blocking of Neutrophils

A murine-specific Cxcr2 blocking antibody was raised in rabbits following immunization with a 17-amino-acid peptide corresponding to the amino terminus of Cxcr2 (Mehrad et al., 1999). Mice were treated with α-Cxcr2 or normal rabbit serum 24 hr prior to infection via intraperitoneal (i.p.) injection as previously described (Walsh et al., 2007).

Extracellular Staining and Flow Cytometry Analysis

Blood neutrophils were detected with phycoerythrin (PE)-conjugated Ly6G (clone RB6-8C5, eBioscience) and PE-Cy7-conjugated CD11b (eBioscience) monoclonal antibodies as described previously (Hosking et al., 2009). Data were acquired on a FACSCalibur (BD Biosciences, San Jose, CA) and analyzed with FlowJo software (TreeStar, Ashland, OR). Leucocytes were gated using forward (FSC) and side scatter (SSC) criteria of cells followed by identification of Ly6G^{high} CD11b$^+$ neutrophils.

Measurement of Zinc in Fecal Samples

The amount of zinc in mouse fecal samples was detected by ICP-MS as described previously (Corbin et al., 2008) and detailed in Supplemental Experimental Procedures.

Analysis of the Microbiota

Composition of the bacterial microbiota was analyzed as described earlier (Barman et al., 2008; Winter et al., 2010). Briefly, the DNA from the colon content was extracted using the QIAamp DNA stool kit (QIAGEN) and used as a template for the q-PCR reaction with the primers described in the Supplemental Experimental Procedures. Gene copy numbers per μl for each sample was determined using the plasmids in the Supplemental Experimental Procedures.

Western Blot

Total protein was extracted from mouse cecum using Tri-Reagent (Molecular Research Center), resolved by SDS-PAGE and transferred to a PVDF membrane. Detection of mouse tubulin was performed with a primary rabbit polyclonal antibody (Cell Signaling Technology), while detection of calprotectin was performed with a polyclonal goat anti-mouse S100a8 and a polyclonal goat anti-mouse S100a9 (R&D Systems). Myeloperoxidase was detected using a primary polyclonal goat anti-human and mouse antibody (R&D Systems). As secondary antibody, a goat anti-rabbit or rabbit anti-goat conjugate to horseradish peroxidase (HRP) (Jackson) was used.

Detection of Intestinal and Fecal Calprotectin Using ELISA

Cecum and colon tissue were placed in 3 ml sterile PBS and homogenized. Extraction buffer adopted from Hycult Biotech's H305 Human Calprotectin ELISA kit was added to fecal samples. The fecal samples were incubated on ice for 30 min and were homogenized at 4°C. Samples were then spun down, and the supernatant was used for western blot and ELISA analyses. Murine S100a8/S100a9 was determined by an inhouse established ELISA as described (Vogl et al., 2007). Recombinant prepared murine S100a8/S100a9 heterodimer was used as standard in the calibration curve. Data were normalized taking into account the weight of the collected fecal samples and tissues and assuming a density of 1g/ml.

Quantitative Real-Time PCR

Total RNA was extracted from mouse cecal tissue using Tri-Reagent (Molecular Research Center). Reverse transcription of 1 μg of total RNA was performed using the Transcriptor First Strand cDNA Synthesis kit (Roche). Quantitative real-time PCR (qRT-PCR) for the expression of β-actin, *Il-17*, *Il-22*, *S100a8*, *S100a9*, *Cxcl-1*, and *Ly6g* was performed with the primers provided in Supplemental Experimental Procedures.

Histopathology

Tissue samples were fixed in formalin, processed according to standard procedures for paraffin embedding, sectioned at 5 μm, and stained with hematoxylin and eosin. The pathology score of cecal samples was determined by blinded examinations of cecal sections from a board-certified pathologist using previously published methods (Barthel et al., 2003; Raffatellu et al., 2009). Each section was evaluated for the presence of neutrophils, mononuclear infiltrate, submucosal edema, surface erosions, inflammatory exudates, and cryptitis. Inflammatory changes were scored from 0 to 4 according to the following scale: 0 = none; 1 = low; 2 = moderate; 3 = high; 4 = extreme. The inflammation score was calculated by adding up all the scores obtained for each parameter and interpreted as follows: 0–2 = within normal limit; 3–5 = mild; 6–8 = moderate; 8+ = severe.

Statistical Analysis

Differences between treatment groups were analyzed by ANOVA followed by Student's t test. A p value equal or below 0.05 was considered statistically significant.

SUPPLEMENTAL INFORMATION

Supplemental Information includes five figures, Supplemental Experimental Procedures, three tables, and Supplemental References and can be found with this article online at doi:10.1016/j.chom.2012.01.017.

REFERENCES

Ammendola, S., Pasquali, P., Pistoia, C., Petrucci, P., Petrarca, P., Rotilio, G., and Battistoni, A. (2007). High-affinity Zn2+ uptake system ZnuABC is required for bacterial zinc homeostasis in intracellular environments and contributes to the virulence of *Salmonella enterica*. Infect. Immun. *75*, 5867–5876.

Barman, M., Unold, D., Shifley, K., Amir, E., Hung, K., Bos, N., and Salzman, N. (2008). Enteric salmonellosis disrupts the microbial ecology of the murine gastrointestinal tract. Infect. Immun. *76*, 907–915.

Barthel, M., Hapfelmeier, S., Quintanilla-Martínez, L., Kremer, M., Rohde, M., Hogardt, M., Pfeffer, K., Rüssmann, H., and Hardt, W.D. (2003). Pretreatment of mice with streptomycin provides a *Salmonella enterica* serovar Typhimurium colitis model that allows analysis of both pathogen and host. Infect. Immun. *71*, 2839–2858.

Campoy, S., Jara, M., Busquets, N., Pérez De Rozas, A.M., Badiola, I., and Barbé, J. (2002). Role of the high-affinity zinc uptake *znuABC* system in *Salmonella enterica* serovar typhimurium virulence. Infect. Immun. *70*, 4721–4725.

Conti, H.R., Shen, F., Nayyar, N., Stocum, E., Sun, J.N., Lindemann, M.J., Ho, A.W., Hai, J.H., Yu, J.J., Jung, J.W., et al. (2009). Th17 cells and IL-17 receptor signaling are essential for mucosal host defense against oral candidiasis. J. Exp. Med. *206*, 299–311.

Corbin, B.D., Seeley, E.H., Raab, A., Feldmann, J., Miller, M.R., Torres, V.J., Anderson, K.L., Dattilo, B.M., Dunman, P.M., Gerads, R., et al. (2008). Metal chelation and inhibition of bacterial growth in tissue abscesses. Science *319*, 962–965.

Davis, L.M., Kakuda, T., and DiRita, V.J. (2009). A *Campylobacter jejuni znuA* orthologue is essential for growth in low-zinc environments and chick colonization. J. Bacteriol. *191*, 1631–1640.

Garrido, M.E., Bosch, M., Medina, R., Llagostera, M., Pérez de Rozas, A.M., Badiola, I., and Barbé, J. (2003). The high-affinity zinc-uptake system *znuACB* is under control of the iron-uptake regulator (fur) gene in the animal pathogen *Pasteurella multocida*. FEMS Microbiol. Lett. *221*, 31–37.

Godinez, I., Haneda, T., Raffatellu, M., George, M.D., Paixão, T.A., Rolán, H.G., Santos, R.L., Dandekar, S., Tsolis, R.M., and Bäumler, A.J. (2008). T cells help to amplify inflammatory responses induced by *Salmonella enterica* serotype Typhimurium in the intestinal mucosa. Infect. Immun. *76*, 2008–2017.

Godinez, I., Raffatellu, M., Chu, H., Paixão, T.A., Haneda, T., Santos, R.L., Bevins, C.L., Tsolis, R.M., and Bäumler, A.J. (2009). Interleukin-23 orchestrates mucosal responses to *Salmonella enterica* serotype Typhimurium in the intestine. Infect. Immun. *77*, 387–398.

Hantke, K. (2001). Bacterial zinc transporters and regulators. Biometals *14*, 239–249.

Hapfelmeier, S., and Hardt, W.D. (2005). A mouse model for *S. typhimurium*-induced enterocolitis. Trends Microbiol. *13*, 497–503.

Hosking, M.P., Liu, L., Ransohoff, R.M., and Lane, T.E. (2009). A protective role for ELR+ chemokines during acute viral encephalomyelitis. PLoS Pathog. *5*, e1000648.

Hunter, M.J., and Chazin, W.J. (1998). High level expression and dimer characterization of the S100 EF-hand proteins, migration inhibitory factor-related proteins 8 and 14. J. Biol. Chem. *273*, 12427–12435.

Johne, B., Fagerhol, M.K., Lyberg, T., Prydz, H., Brandtzaeg, P., Naess-Andresen, C.F., and Dale, I. (1997). Functional and clinical aspects of the myelomonocyte protein calprotectin. MP, Mol. Pathol. *50*, 113–123.

Kehl-Fie, T.E., and Skaar, E.P. (2010). Nutritional immunity beyond iron: a role for manganese and zinc. Curr. Opin. Chem. Biol. *14*, 218–224.

Kehl-Fie, T.E., Chitayat, S., Hood, M.I., Damo, S., Restrepo, N., Garcia, C., Munro, K.A., Chazin, W.J., and Skaar, E.P. (2011). Nutrient metal sequestration by calprotectin inhibits bacterial superoxide defense, enhancing neutrophil killing of *Staphylococcus aureus*. Cell Host Microbe *10*, 158–164.

Kim, S., Watanabe, K., Shirahata, T., and Watarai, M. (2004). Zinc uptake system (*znuA* locus) of *Brucella abortus* is essential for intracellular survival and virulence in mice. J. Vet. Med. Sci. *66*, 1059–1063.

Konikoff, M.R., and Denson, L.A. (2006). Role of fecal calprotectin as a biomarker of intestinal inflammation in inflammatory bowel disease. Inflamm. Bowel Dis. *12*, 524–534.

Lawley, T.D., Bouley, D.M., Hoy, Y.E., Gerke, C., Relman, D.A., and Monack, D.M. (2008). Host transmission of *Salmonella enterica* serovar Typhimurium is controlled by virulence factors and indigenous intestinal microbiota. Infect. Immun. *76*, 403–416.

Lewis, D.A., Klesney-Tait, J., Lumbley, S.R., Ward, C.K., Latimer, J.L., Ison, C.A., and Hansen, E.J. (1999). Identification of the *znuA*-encoded periplasmic zinc transport protein of *Haemophilus ducreyi*. Infect. Immun. *67*, 5060–5068.

Liang, S.C., Tan, X.Y., Luxenberg, D.P., Karim, R., Dunussi-Joannopoulos, K., Collins, M., and Fouser, L.A. (2006). Interleukin (IL)-22 and IL-17 are coexpressed by Th17 cells and cooperatively enhance expression of antimicrobial peptides. J. Exp. Med. *203*, 2271–2279.

Loomans, H.J., Hahn, B.L., Li, Q.Q., Phadnis, S.H., and Sohnle, P.G. (1998). Histidine-based zinc-binding sequences and the antimicrobial activity of calprotectin. J. Infect. Dis. *177*, 812–814.

Lupp, C., Robertson, M.L., Wickham, M.E., Sekirov, I., Champion, O.L., Gaynor, E.C., and Finlay, B.B. (2007). Host-mediated inflammation disrupts the intestinal microbiota and promotes the overgrowth of *Enterobacteriaceae*. Cell Host Microbe *2*, 204.

Lusitani, D., Malawista, S.E., and Montgomery, R.R. (2003). Calprotectin, an abundant cytosolic protein from human polymorphonuclear leukocytes, inhibits the growth of *Borrelia burgdorferi*. Infect. Immun. *71*, 4711–4716.

Manitz, M.P., Horst, B., Seeliger, S., Strey, A., Skryabin, B.V., Gunzer, M., Frings, W., Schönlau, F., Roth, J., Sorg, C., and Nacken, W. (2003). Loss of S100A9 (MRP14) results in reduced interleukin-8-induced CD11b surface expression, a polarized microfilament system, and diminished responsiveness to chemoattractants in vitro. Mol. Cell. Biol. *23*, 1034–1043.

Mehrad, B., Strieter, R.M., Moore, T.A., Tsai, W.C., Lira, S.A., and Standiford, T.J. (1999). CXC chemokine receptor-2 ligands are necessary components of neutrophil-mediated host defense in invasive pulmonary aspergillosis. J. Immunol. *163*, 6086–6094.

Nielubowicz, G.R., Smith, S.N., and Mobley, H.L. (2010). Zinc uptake contributes to motility and provides a competitive advantage to *Proteus mirabilis* during experimental urinary tract infection. Infect. Immun. *78*, 2823–2833.

Noriega, L.M., Van der Auwera, P., Daneau, D., Meunier, F., and Aoun, M. (1994). *Salmonella* infections in a cancer center. Support. Care Cancer *2*, 116–122.

Raffatellu, M., Santos, R.L., Verhoeven, D.E., George, M.D., Wilson, R.P., Winter, S.E., Godinez, I., Sankaran, S., Paixao, T.A., Gordon, M.A., et al. (2008). Simian immunodeficiency virus-induced mucosal interleukin-17 deficiency promotes *Salmonella* dissemination from the gut. Nat. Med. *14*, 421–428.

Raffatellu, M., George, M.D., Akiyama, Y., Hornsby, M.J., Nuccio, S.P., Paixao, T.A., Butler, B.P., Chu, H., Santos, R.L., Berger, T., et al. (2009). Lipocalin-2 resistance confers an advantage to *Salmonella enterica* serotype Typhimurium for growth and survival in the inflamed intestine. Cell Host Microbe *5*, 476–486.

Rohmer, L., Hocquet, D., and Miller, S.I. (2011). Are pathogenic bacteria just looking for food? Metabolism and microbial pathogenesis. Trends Microbiol. *19*, 341–348.

Sabri, M., Houle, S., and Dozois, C.M. (2009). Roles of the extraintestinal pathogenic *Escherichia coli* ZnuACB and ZupT zinc transporters during urinary tract infection. Infect. Immun. *77*, 1155–1164.

Santos, R.L., Raffatellu, M., Bevins, C.L., Adams, L.G., Tükel, C., Tsolis, R.M., and Bäumler, A.J. (2009). Life in the inflamed intestine, *Salmonella* style. Trends Microbiol. *17*, 498–506.

Sohnle, P.G., Hunter, M.J., Hahn, B., and Chazin, W.J. (2000). Zinc-reversible antimicrobial activity of recombinant calprotectin (migration inhibitory factor-related proteins 8 and 14). J. Infect. Dis. *182*, 1272–1275.

Srinivasan, A., Salazar-Gonzalez, R.M., Jarcho, M., Sandau, M.M., Lefrancois, L., and McSorley, S.J. (2007). Innate immune activation of CD4 T cells in *salmonella*-infected mice is dependent on IL-18. J. Immunol. *178*, 6342–6349.

Stecher, B., Robbiani, R., Walker, A.W., Westendorf, A.M., Barthel, M., Kremer, M., Chaffron, S., Macpherson, A.J., Buer, J., Parkhill, J., et al. (2007). *Salmonella enterica* serovar typhimurium exploits inflammation to compete with the intestinal microbiota. PLoS Biol. *5*, 2177–2189.

Steinbakk, M., Naess-Andresen, C.F., Lingaas, E., Dale, I., Brandtzaeg, P., and Fagerhol, M.K. (1990). Antimicrobial actions of calcium binding leucocyte L1 protein, calprotectin. Lancet *336*, 763–765.

Teigelkamp, S., Bhardwaj, R.S., Roth, J., Meinardus-Hager, G., Karas, M., and Sorg, C. (1991). Calcium-dependent complex assembly of the myeloic differentiation proteins MRP-8 and MRP-14. J. Biol. Chem. *266*, 13462–13467.

Tsolis, R.M., Adams, L.G., Ficht, T.A., and Bäumler, A.J. (1999). Contribution of *Salmonella typhimurium* virulence factors to diarrheal disease in calves. Infect. Immun. *67*, 4879–4885.

Urban, C.F., Ermert, D., Schmid, M., Abu-Abed, U., Goosmann, C., Nacken, W., Brinkmann, V., Jungblut, P.R., and Zychlinsky, A. (2009). Neutrophil extracellular traps contain calprotectin, a cytosolic protein complex involved in host defense against *Candida albicans*. PLoS Pathog. *5*, e1000639.

Vogl, T., Tenbrock, K., Ludwig, S., Leukert, N., Ehrhardt, C., van Zoelen, M.A., Nacken, W., Foell, D., van der Poll, T., Sorg, C., and Roth, J. (2007). Mrp8 and Mrp14 are endogenous activators of Toll-like receptor 4, promoting lethal, endotoxin-induced shock. Nat. Med. *13*, 1042–1049.

Walsh, K.B., Edwards, R.A., Romero, K.M., Kotlajich, M.V., Stohlman, S.A., and Lane, T.E. (2007). Expression of CXC chemokine ligand 10 from the mouse hepatitis virus genome results in protection from viral-induced neurological and liver disease. J. Immunol. *179*, 1155–1165.

Whitehead, R.H., VanEeden, P.E., Noble, M.D., Ataliotis, P., and Jat, P.S. (1993). Establishment of conditionally immortalized epithelial cell lines from both colon and small intestine of adult H-2Kb-tsA58 transgenic mice. Proc. Natl. Acad. Sci. USA *90*, 587–591.

Winkelstein, J.A., Marino, M.C., Johnston, R.B., Jr., Boyle, J., Curnutte, J., Gallin, J.I., Malech, H.L., Holland, S.M., Ochs, H., Quie, P., et al. (2000). Chronic granulomatous disease. Report on a national registry of 368 patients. Medicine (Baltimore) *79*, 155–169.

Winter, S.E., Thiennimitr, P., Winter, M.G., Butler, B.P., Huseby, D.L., Crawford, R.W., Russell, J.M., Bevins, C.L., Adams, L.G., Tsolis, R.M., et al. (2010). Gut inflammation provides a respiratory electron acceptor for *Salmonella*. Nature *467*, 426–429.

Zaia, A.A., Sappington, K.J., Nisapakultorn, K., Chazin, W.J., Dietrich, E.A., Ross, K.F., and Herzberg, M.C. (2009). Subversion of antimicrobial calprotectin (S100A8/S100A9 complex) in the cytoplasm of TR146 epithelial cells after invasion by *Listeria monocytogenes*. Mucosal Immunol. *2*, 43–53.

Zheng, Y., Valdez, P.A., Danilenko, D.M., Hu, Y., Sa, S.M., Gong, Q., Abbas, A.R., Modrusan, Z., Ghilardi, N., de Sauvage, F.J., and Ouyang, W. (2008). Interleukin-22 mediates early host defense against attaching and effacing bacterial pathogens. Nat. Med. *14*, 282–289.